The Open Materials Science Journal, 2014, *8*, 31-38

Synergistic Inhibition Effect Between *Capsella bursa-pastoris* Extracts and Iodide Ions for Q235 Mild Steel in 1 M HCl Solution

Qin Hu[1], Yubing Qiu[1], Guoan Zhang[1] and Xingpeng Guo[*,1,2]

[1]*School of Chemistry and Chemical Engineering, Huazhong University of Science and Technology, Wuhan 430074, China*

[2]*Hubei Key Laboratory of Materials Chemistry and Service Failure, Wuhan 430074, China*

Abstract: The inhibition effect of *Capsella bursa-pastoris* extracts (CBE) and its synergistic effect with KI (CBEK) for Q235 mild steel in 1 M HCl solution were studied by electrochemical measurements. Both CBE and CBEK can serve as eco-friendly, mixed-type inhibitors, and the inhibition efficiency increases with the concentration and temperature. The synergistic parameter (S_I) indicates a cooperative mechanism between the iodide anions and CBE molecules at lower temperature. The associated thermodynamic and kinetic data suggest the presence of CBEK on metal surface mainly through chemisorption at higher temperature. The adsorption processes follow Langmuir isotherm.

Keywords: Acid corrosion, electrochemical calculation, electrochemical techniques, mild steel, synergistic inhibition.

INTRODUCTION

It is well known that metal corrosion will result in the degradation and eventual failure of components and systems in the processing and manufacturing industries, which needs to be controlled or prevented by some methods, such as the barrier protection, galvanization, cathodic protection and inhibitors. Among these methods, using inhibitors, which can reduce the attack on metals by adding small amounts to the environment, is very popular. However, most of the synthetic inhibitors are expensive and highly toxic to the living systems. To avoid this situation, new class of natural inhibitors, which are extracted from nature plants, should be developed. Plant extracts, which can be obtained through simple extraction process, are generally low toxicity, eco-friendliness and inexpensive. Therefore, there has been a growing trend to try to find efficient and readily available inhibitors in natural products [1-6].

Generally, if two or more inhibitors are added to the same corrosive system, the inhibition effect may be much greater than the individual effect of each inhibitor, which can be called the synergistic effect [7]. Synergistic inhibition has been proven to be an effective means of improving the inhibitive efficiency, decreasing the amount of usage and diversifying the application of inhibitor. For example, halide ions either stimulate or inhibit the corrosion of metals, depending on the concentration. A high synergistic effect of iodide ions was reported through chemisorption on metal surface due to its larger size and ease of polarizability [8]. It is widely known that halide ions have synergistic effect with many organic compounds such as amines, amides, imidazolines or quaternary ammonium salts, which are strongly polar functional compounds and contain P, S, and O [9]. However, there are only a few studies on the synergistic effect of halide ions and plant extract.

Capsella bursa-pastoris, commonly known as shepherd's purse, is a wild plant, whose young leaves and roots are edible vegetables in China. Its chemical composition, including minerals, vitamin A, ascorbic acid, proteins, linoleic acid and fatty acids, is considered to be beneficial to human health [10, 11]. Besides the good nutritional value, *Capsella bursa-pastoris* presents important biological properties and medicinal properties, being used for anti-bleeding, anticancer [12], wound-healing and antioxidant agent [13], as well as for diabetes and fever treatment. The CBE contains mixtures of organic compounds in nature, which having nitrogen, sulfur, triple bonds and aromatic rings as effective inhibition function groups. In this study, the inhibitive effect of *Capsella bursa-pastoris* extract (CBE) and its synergistic inhibition effect with iodide ions (CBEK) on the corrosion of Q235 mild steel in HCl solution were studied by potentiodynamic polarization and electrochemical impedance spectroscopy (EIS) measurements. The inhibitive performance, adsorption behaviour, co-adsorption mechanism and synergistic effect were determined.

MATERIALS AND METHODOLOGY

Preparation of the electrodes

Q235 mild steel, with the chemical composition shown in Table **1**, was machined into specimens with the dimensions of 1 × 1 × 0.6 cm. A copper wire was soldered to each specimen to ensure electrical connection for electrochemical measurements. Then the specimens were mounted in PVC holder and embedded with epoxy resin with the exposed area of 1 cm^2. The exposed surface of each specimen was ground with silicon carbide abrasive paper up to 1200 grits, and then

---

*Address correspondence to this author at the School of Chemistry and Chemical Engineering, Huazhong University of Science and Technology, Wuhan 430074, China; Tel.: +86-27-87543432; Fax: +86-27-87543632; E-mail: guoxp@mail.hust.edu.cn

1874-088X/14

Table 1. Chemical composition of Q235 mild steel.

Element	C	Si	Mn	P	S	Al	Ni	Cr	Cu
Composition (wt %)	0.18	0.07	0.28	0.016	0.006	--	0.01	0.02	0.05

rinsed with double-distilled water, degreased with ethanol and acetone.

Preparation of Solution

The testing solution was 1 M HCl, which was made up from analytical grade reagent and deionized water. The air-dried aerial parts of *Capsella bursa-pastoris* was powdered in particle size lower than 0.3 mm. The *Capsella bursa-pastoris* inhibitor was extracted by adding some powders to 50% ethanol + 50% water solution for 45 min under ultrasonic condition. These extract conditions were optimized by primordial orthogonal experiments. KI with various concentrations (0.01–100 mM) was added to the solution to determine the inhibition efficiency of KI and the synergistic inhibition effect of *Capsella bursa-pastoris* and KI.

Electrochemical Measurements

Electrochemical measurements were carried out in a conventional three-electrode glass cell by using an electrochemical test system (CS350, China). A platinum foil was used as the counter electrode and a saturated calomel electrode (SCE), which was connected to the cell externally through a Luggin capillary tube, was served as reference electrode. All the potentials reported here were referred to this reference electrode. Polarization curves were measured from -0.25 V to 0.25 V *vs* open circuit potential (OCP) with a constant sweep rate of 0.5 mV/s. EIS was recorded over the frequency range of 100 kHz to 10 mHz at OCP when OCP reached steady status (within ±1 mV min^{-1}). From the calculated values of charge transfer resistance (R_{ct}) and corrosion current density (i_{corr}), the inhibition efficiency (η%) was calculated from the following Eqs. (1, 2):

$$\eta\% = [(R'_{ct} - R_{ct}) / R'_{ct}] \times 100 \qquad (1)$$

$$\eta\% = [(i_{corr} - i'_{corr}) / i_{corr}] \times 100 \qquad (2)$$

where R_{ct} (uninhibited systems) and R'_{ct} (inhibited systems) are the charge transfer resistances calculated from EIS, while i_{corr} (uninhibited systems) and i'_{corr} (inhibited systems) are the corrosion current densities calculated from Tafel polarization, respectively.

RESULTS

Electrochemical Impedance Spectroscopy (EIS) Measurements

Fig. (**1**) shows the Nyquist plots of Q235 mild steel in 1 M HCl solution in absence and presence of KI and CBEK at 25°C. It is seen that all the Nyquist plots are characterized by one depressed capacitive semicircle. This depressed capacitive semicircle should be attributed to the heterogeneity of electrode surface [14, 15]. The diameter of the capacitive semicircle increases, *i.e.*, an increase in the inhibition efficiency, with increasing KI concentration. Furthermore, the diameter of the capacitive semicircle in coexistence of KI and CBE is much larger than that of each individual inhibitor, indicating the synergistic effect of KI and CBE.

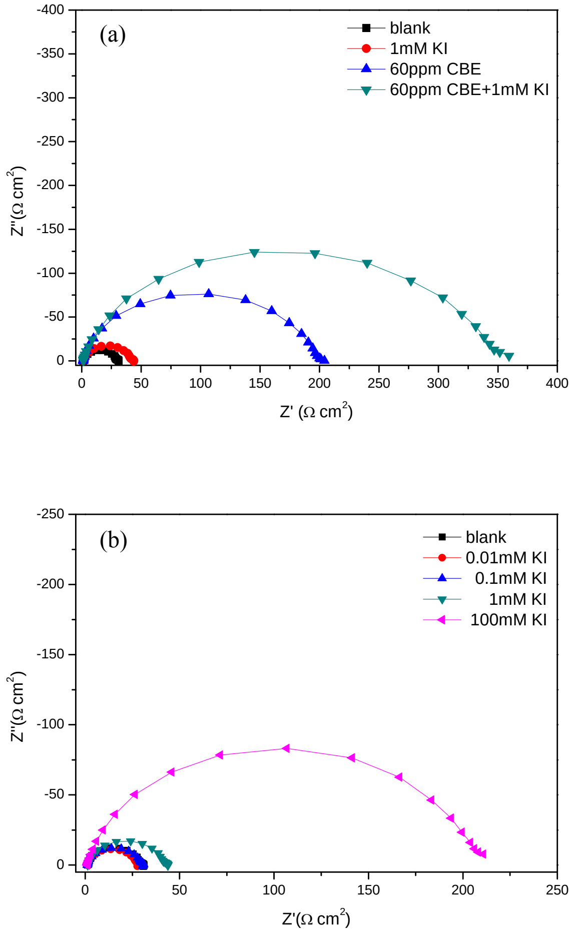

Fig. (1). Nyquist plots for Q235 mild steel in 1 M HCl solution (**a**) in the presence of CBE, KI and CBEK, (**b**) in the presence of different concentrations of KI at 25°C.

To analyze and obtain the impedance parameters, an electrochemical equivalent circuit shown in Fig. (**2**) was used for fitting the EIS data, where R_s is solution resistance, CPE is constant phase element, R_{ct} is charge transfer resistance. The corresponding fitted values of impedance parameters are listed in Table **2**. It should be pointed out that the value of C_{dl} was obtained by converting the constant phase element parameter (Y_0) with following equation [16, 17]:

$$C_{dl} = (\text{CPE-T} \times R_{ct})^{1/\text{CPE-P}} / R_{ct} \qquad (3)$$

where CPE-T is the frequency independent admittance; CPE-P is the power of Y_0. From Table **2**, it is seen that the value of R_{ct} in coexistence of KI and CBE is larger than that

Table 2. EIS fitted parameters for Q235 mild steel in 1 M HCl and in the presence of CBE, KI or CBEK at 25°C.

c_{CBE} (ppm)	c_{KI} (mM)	R_s ($\Omega \mathrm{cm}^2$)	R_{ct} ($\Omega \mathrm{cm}^2$)	CPE-T	CPE-P	C_{dl} (μF cm^{-2})	η (%)
0	0	1.3	29.1	251.8	0.90	146.6	--
0	0.01	1.2	26.7	236.7	0.90	133.1	-8.25
0	0.1	1.2	29.1	234.5	0.90	130.5	0.10
0	1	1.4	41.3	194.3	0.89	109.1	29.59
0	100	1.1	211.4	103.3	0.88	60.2	86.23
60	0	1.3	195.4	90.2	0.89	55.2	85.11
60	0.01	1.1	236.7	101.5	0.87	58.1	87.71
60	0.1	1.4	226.4	94.1	0.88	55.2	87.15
60	1	1.3	344.0	82.2	0.86	45.7	91.54

in the individual presence of CBE or KI, which indicates the higher inhibition efficiency of CBEK compared to CBE or KI. Furthermore, the value of R_{ct} in the presence of KI is larger than that in the absence of KI. The value of R_{ct} increases while the value of C_{dl} decreases with increasing KI concentration. It is obvious that the adsorption extent of iodide ions on the metal/solution interface affects the value of C_{dl}. The interfacial capacitance in the presence of KI may be expressed as follows:

$$C_c = \theta C_s + (1-\theta) C_0 \tag{4}$$

$$u = \lambda \theta \tag{5}$$

where $u = 1 - C_c / C_0$, $\lambda = 1 - C_s / C_0$; θ is the surface coverage which can be evaluated from the expression: $\eta\% = \theta \times 100$; C_0 is the interfacial capacitance in the absence of KI, and C_c is the interfacial capacitance in the presence of KI; C_s is the interfacial capacitance when θ equals to 1.

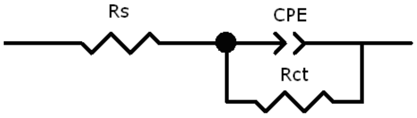

Fig. (2). Equivalent electrical circuit of the interface of mild steel / HCl solution both in the absence and presence of CBE or CBEK.

Plotting u against θ gives a straight line, as shown in Fig. (**3**). Then C_s can be calculated from the slope. The obtained C_s was between 70 and 60 μ F cm^{-2}. The decrease in C_{dl} with increasing KI concentration indicates that the iodide ions adsorb on the metal/solution interface and replace H_2O molecules. As shown in Table **2**, the value of C_{dl} is less than 60 μ F cm^{-2} in the coexistence of KI and CBE, and the inhibition efficiency is higher in the coexistence system than that in the presence of KI or CBE. This suggests that CBE molecules also replace H_2O molecules and directly adsorb on the metal surface.

Fig. (**4**) shows the inhibition efficiencies of CBE and CBEK for Q235 mild steel after immerged in 1 M HCl solution for different times at 25°C. The inhibition efficiency increases with the prolongation of immersion time for both inhibitors. The inhibition efficiency is higher in the presence of CBEK than that in the presence of CBE. Furthermore, compared to the inhibition efficiency of CBE, it takes shorter time for the inhibition efficiency to reach a stable value in the coexistence of KI and CBE, which may be due to the synergistic effect between CBE molecules and iodide anions.

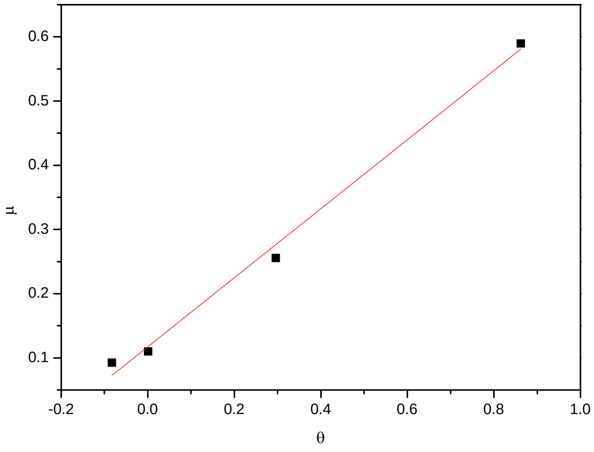

Fig. (3). A plot of u *versus* θ for the adsorption of iodide ions.

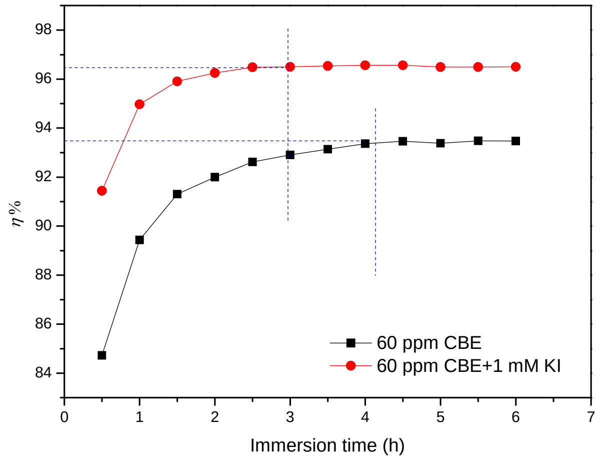

Fig. (4). Time dependence of the inhibition efficiencies of CBE and CBEK for Q235 mild steel in 1 M HCl solution at 25°C.

POTENTIODYNAMIC POLARIZATION CURVES MEASUREMENTS

Fig. (**5**) shows the polarization curves of Q235 mild steel in 1 M HCl solution in the presence of CBE and/or KI at 25°C. It can be seen that the presence of CBE causes a decrease in both anodic and cathodic current densities. The anodic and cathodic current densities further decrease with adding 2.5 mM KI suggests that both CBE and CBK are mixed-type inhibitors. Furthermore, there is no significant change (less than 85 mV) in the corrosion potential in the presence of CBE and KI [18].

To assess the influence of temperature and inhibitor concentration on inhibition efficiency, potentiodynamic polarization curves measurements were carried out at 25°C and 35°C with different concentrations of CBE. The values of corresponding parameters for polarization curves, such as corrosion potential (E_{corr}), corrosion current density (i_{corr}), anodic and cathodic Tafel slope (b_a, b_c) listed in Table **3**, are obtained by fitting data measured in $\pm 80 \sim \pm 150$mV *vs* E_{corr} using professional software installed in the electrochemical test system. It is seen that the corrosion current density increases with the increase of temperature in both the uninhibited and inhibited solutions. However, the inhibition efficiency of CBE or CBEK increases with increasing temperature and concentration. Furthermore, inhibition efficiency of CBEK is higher than that of CBE, as shown in Fig. (**6**), which indicates a synergistic effect of these two inhibitors.

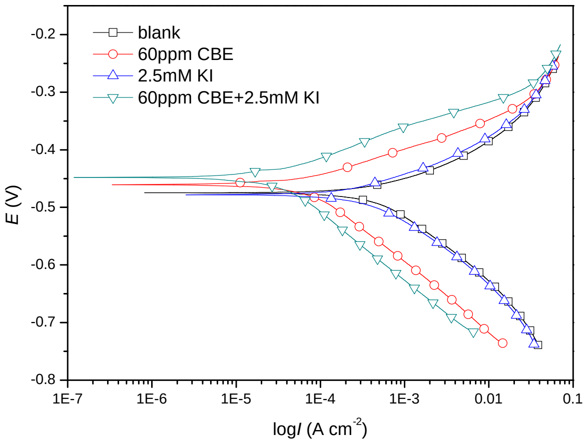

Fig. (5). Polarization curves of Q235 mild steel in 1 M HCl solution in the presence of CBE, KI and CBEK 25°C.

ADSORPTION AND DESORPTION BEHAVIORS OF CBE AND CBEK

It is acknowledged that the adsorption behavior of an inhibitor can be analyzed by the adsorption mechanism,

Table 3. Potentiodynamic polarization parameters for Q235 mild steel in 1 M HCl and in the presence of CBE or CBEK at 25°C and 35°C.

T (°C)	c CBE (ppm)	c KI (mM)	$-E_{corr}$ (mV)	b_a (mV)	$-b_c$ (mV)	i_{corr} (µA cm^{-2})	η (%)	S_I
25	0	0	493.1	70.9	100.4	441.2	--	--
	0	2.5	486.9	66.6	100.0	364.3	17.44	--
	20	0	483.9	56.7	104.8	143.7	67.43	--
	40	0	483.0	53.6	107.5	103.9	76.44	--
	60	0	484.5	40.6	109.5	50.5	88.55	--
	80	0	484.1	46.7	120.5	60.5	86.30	--
	20	2.5	480.5	45.5	104.6	57.2	87.03	2.07
	40	2.5	468.5	49.8	124.9	37.4	91.52	2.29
	60	2.5	471.1	59.1	121.6	31.5	92.85	1.32
	80	2.5	470.1	59.4	154.3	31.4	92.88	1.59
35	0	0	489.7	54.4	96.2	760.0	0	--
	0	2.5	479.6	50.5	91.4	391.8	48.45	--
	20	0	481.5	41.2	104.2	234.5	69.14	--
	40	0	479.9	35.9	106.8	104.5	86.25	--
	60	0	476.4	41.5	119.0	68.5	90.99	--
	80	0	480.1	41.9	107.8	65.9	91.33	--
	20	2.5	471.6	48.9	106.9	59.9	92.11	2.02
	40	2.5	464.8	59.6	113.5	44.4	94.16	1.21
	60	2.5	459.0	60.9	118.7	41.8	94.50	0.84
	80	2.5	463.6	66.0	135.5	38.2	94.97	0.89

assuming a direct relationship between the inhibition efficiency (η %) and the coverage of inhibitor (θ). Fig. (**7**) shows a linear relationship of c/θ versus c with a proximate slope of unity and a high regression correlation coefficient (0.99). This suggests that the adsorption of CBE and CBEK on steel surface follows the Langmuir isotherm [19], which may be expressed as follows:

$$c/\theta = 1/K + c \qquad (6)$$

where K is adsorption equilibrium constant (L mg^{-1}).

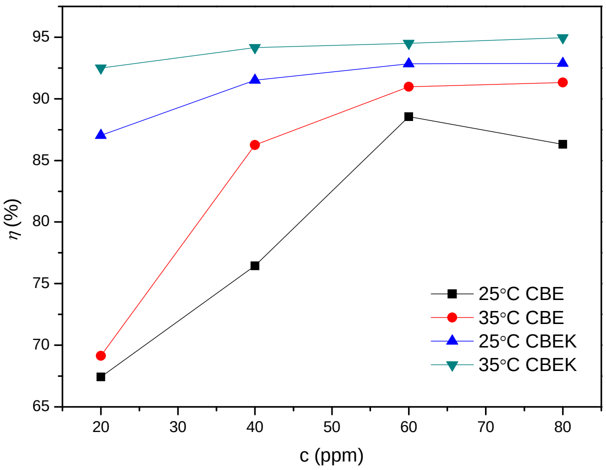

Fig. (6). Inhibition efficiencies of CBE or CBEK for Q235 mild steel in 1 M HCl solution at 25°C and 35°C.

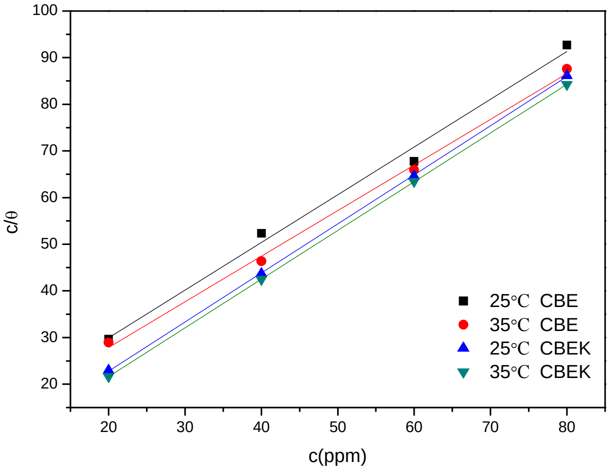

Fig. (7). Langmuir adsorption isotherm model for CBE and CBEK on Q235 mild steel surface.

To study the desorption behavior of CBEK inhibitor, differential polarization curve method was applied to the anodic polarization curve data [20].

$$S = d\lg i/dE \qquad (7)$$

where S is the reciprocal of the slope of every point on semilog polarization curve, and the S versus E is the differential polarization curve, as shown in Fig. (**8**). E_{des} is the desorption potential and E_p is the potential corresponding to the peak of the inhibitor desorption [21]. It is observed that there are positive shifts in both the E_{des} and E_p with increasing CBE concentration at each temperature. Furthermore, the value of S is higher at 35 °C than that at 25 °C indicating that the desorption behavior of inhibitor is more prominent at 35 °C than that at 25 °C. Fig. (**9**) shows a half logarithm relationship between E_{des} and CBE concentration (c), which probably suggests that the CBE concentration influence the value of E_{des}, i.e., the CBE molecules can directly adsorb on the metal surface and then enhance the inhibition efficiency [20].

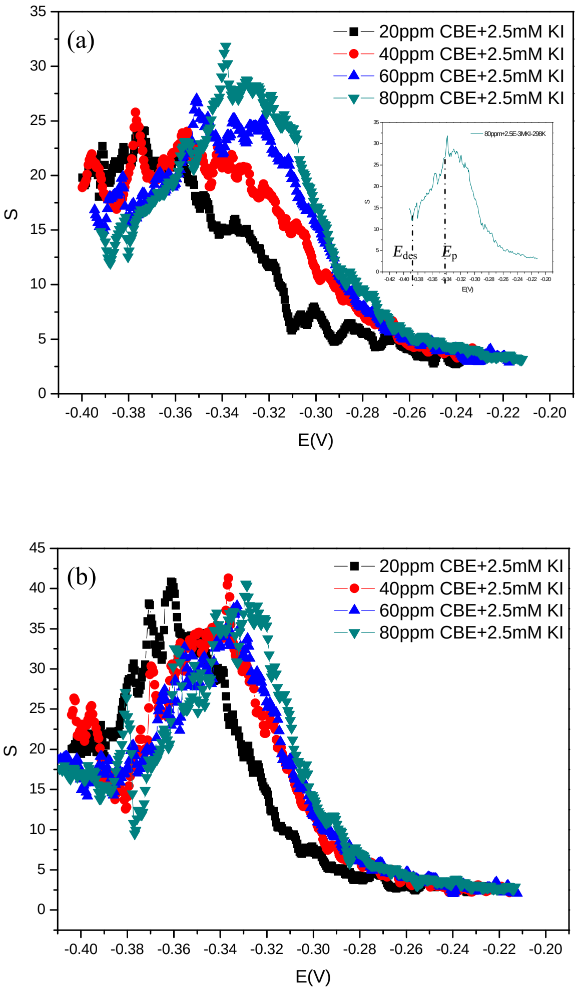

Fig. (8). The anodic differential polarization curve of Q235 mild steel in 1 M HCl solution in the presence of CBEK at (**a**) 25°C, (**b**) 35°C.

THERMODYNAMIC AND KINETIC PARAMETERS

It is well known that the inhibition efficiency and adsorption process of inhibitor can be evaluated by the thermodynamic and kinetic parameters. The equilibrium constant of adsorption is related to the standard free energy of adsorption, ΔG_{ads} by:

$$K = \{\exp[(-\Delta G_{ads})/RT]\}/c_{solvent} \qquad (8)$$

where $c_{solvent}$ represents the concentration of water in solution with the value of approximate 1.0 ×10^6, which results from the unit of K (L mg^{-1}) [22]. Table **4** lists the standard free

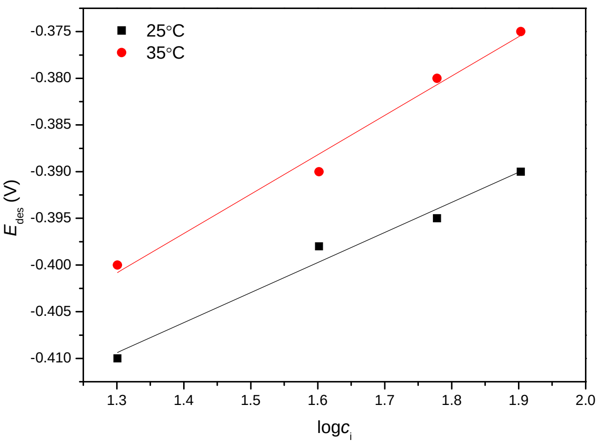

Fig. (9). The linear relationship between E_{des} and CBE concentrations (c_i).

energy of adsorption (ΔG_{ads}) of CBE with and without KI at 25°C and 35°C. It can be seen that both the ΔG_{ads} values in inhibited systems are negative, suggesting the spontaneity of the adsorption process and the stability of the adsorbed inhibitor layer on the steel surface. The variation trend of ΔG_{ads} values is associated with the inhibition efficiency, i.e., the value of ΔG_{ads} increases with temperature and a higher value in CBEK synergistic inhibited system compared to CBE alone inhibited system. Generally, ΔG_{ads} values more negative than −40 kJ mol^{-1} involve charge sharing or transfer from the inhibitor molecules to the metal surface to form a coordinate type of bond (chemisorption), and ΔG_{ads} values of approximately −20 kJ mol^{-1} or lower indicate the electrostatic attraction between the charged metal surface and the charged organic molecules in the solution [23]. Furthermore, a value of ΔG_{ads} between −20 kJ mol^{-1} and −40 kJ mol^{-1} indicates two types of adsorption on the metal surface, i.e., physical adsorption and chemisorption. And chemisorption plays a more important role increasing with temperature.

Table 4. The free energy of adsorption (ΔG_{ads}) of CBE with and without KI at 25°C and 35°C.

T (°C)	c_{KI} (mM)	*K* (L mg^{-1})	ΔG_{ads} (kJ mol^{-1})
25	0	0.106	-28.66
35	0	0.120	-29.96
25	2.5	0.566	-32.82
35	2.5	1.341	-36.13

The values of apparent activation energy (E_a), heat of adsorption (Q_{ads}), can be calculated using the following equations (9, 10) [24]:

$$i_{corr} = A\exp[(-E_a)/RT] \tag{9}$$

$$Q_{ads} = 2.303R\left[\log\left(\frac{\theta_2}{1-\theta_2}\right) - \log\left(\frac{\theta_1}{1-\theta_1}\right)\right]\times\left(\frac{T_1\times T_2}{T_2-T_1}\right) \tag{10}$$

where θ_1 and θ_2 are degree of surface coverage at temperature T_1 and T_2, respectively. Table **5** lists the values of $\triangle E_a$ and Q_{ads} for the corrosion of Q235 mild steel in 1 M HCl solution without and with CBE or CBEK between 25°C and 35°C, respectively. It is found that the E_a value in the inhibited system is lower than that in the uninhibited system. The reduction of E_a in the presence of inhibitor may be attributed to the chemisorption of inhibitor on the steel surface [25-27]. With the increase of temperature, some chemical changes occur in the inhibitor molecules, leading to an increment in the electron densities at the adsorption centre of inhibitor molecules and then an improvement in inhibition efficiency. Moreover, the E_a in the coexistence of CBE and KI is much lower than that in the inhibited system of CBE alone. It is also seen that the Q_{ads} values are positive in all the cases. The positive value of Q_{ads} may suggest the presence of chemisorption adsorption [28]. The variation trend of Q_{ads} is associated with the inhibition efficiency, i.e., Q_{ads} increases with temperature and a higher value in CBE and KI synergistic inhibited system compared to CBE alone inhibited system.

Table 5. Values of E_a (kJ mol^{-1}) and Q_{ads} (kJ mol^{-1}) for Q235 mild steel in 1 M HCl solution without and with CBE or CBEK.

Conditions	E_a (kJ mol^{-1})	Q_{ads} (kJ mol^{-1})
Blank	41.99	0
CBE	17.08	28.99
CBEK	13.42	30.63

DISCUSSION

Generally, for the interaction of inhibitors A and B, the synergism parameter (S_I) is defined as follows [29]:

$$S_I = (1-\eta_A-\eta_B+\eta_A\eta_B)/(1-\eta_{A+B}) \tag{11}$$

where η_a and η_B are the inhibition efficiencies of inhibitors A and B, respectively, and η_{A+B} is the inhibition efficiency for the combination of inhibitors A and B. Generally, S_I approaches 1 when inhibitors A and B have no interaction on each other at the metal /solution interface, while $S > 1$ indicates a synergistic effect. In the case of $S < 1$, antagonistic effect prevails, which may be attributed to competitive adsorption. The calculated values of S_I for different CBE concentrations with certain iodide ions concentration are listed in Table **3**. It is seen that the value of S_I is more than unity and decreasing with rise in concentration at 25°C, which suggests a synergistic effect between CBE and KI, and the effect weakens at higher CBE concentration. And the variation of S_I at 35°C is the same with that at 25°C. However, S_I decreases to below unity when CBE concentration reaches 60 ppm at 35°C. This maybe due to the easier adsorption of CBE onto the steel surface when the concentration and temperature increasing.

In the absence of iodide ions, the inhibitive action of CBE is due to the composition of numerous organic compounds [30-32], which contain oxygen and nitrogen atoms in functional groups (O–H, C–N, C=C, C–O–C) and an aromatic ring. These chemical compounds meet the general consideration of typical corrosion inhibitors [28], and may react with the ferrous ions, which result from the dissolution of steel (anodic reaction) [33], to form organo-metallic complex such as [Fe-CBE] to reduce hydrogen evolution reaction (cathodic reaction) according to the following mechanism [34]:

$$\mathrm{Fe}_{M} \rightleftharpoons \mathrm{Fe}^{2+}_{sol} + 2e_{M} \qquad (12)$$

$$\mathrm{Fe} + \mathrm{CBE} \rightarrow [\mathrm{Fe} - \mathrm{CBE}] \qquad (13)$$

At the same time, it is well known that the steel surface charges positive charge in acid solution and most plant molecules can be protonated in the acid medium as follows:

$$\mathrm{CBE} + x\mathrm{H}^{+} \rightarrow [\mathrm{CBEH}_{x}]^{x+} \qquad (14)$$

In this case, it would be difficult for the protonated CBE molecules to approach the positively charged steel surface because of electrostatic repulsion. However, in the presence of iodide ions, the anions are specifically adsorbed on the steel surface due to the smaller degree of hydration, which allows the protonated CBE molecules to easily approach the steel surface [35, 36]. The protonated CBE may adsorb on the steel surface through iodide ions to form organo - iodide - metallic complex such as $[\text{Fe-I-CBEH}_x]^{x-1}$ according to the following mechanism:

$$[\mathrm{CBEH}_{x}]^{x+} + \mathrm{I}^{-} + \mathrm{Fe} \rightarrow [\mathrm{Fe} - \mathrm{I} - \mathrm{CBEH}_{x}]^{x-1} \qquad (15)$$

Thus, in the coexistence of CBE and iodide ions, two adsorption modes [Fe-CBE], and $[\text{Fe-I-CBEH}_x]^{x-1}$, should account for the synergistic inhibition effect. These complexes might adsorb on steel surface mainly through chemisorption, while electrostatic interaction and van der Waals force also play a role in forming a stable protective film, resulting in an inhibitive effect [37, 38].

CONCLUSION

Capsella bursa-pastoris extracts (CBE) can be used as an effective, eco-friendly inhibitor for mild steel in acid environment.

The inhibition efficiency is further enhanced in the coexistence of CBE and KI (CBEK), and it takes shorter time for the inhibition efficiency to reach a stable value in the presence of CBEK compared to CBE, which may be due to the synergistic effect between CBE molecules and iodide anions *i.e.*, the protonated CBE adsorb on negatively charged metal surface after adsorbing iodide ions.

Both CBE and CBEK act as mix-type inhibitors. The inhibition efficiency increases with the concentration, temperature and immersion time. The differential polarization curves suggest that both the desorption potential (E_{des}) and the peak potential (E_{p}) shift positively with increasing CBE concentration and temperature, i.e., a more stable protective film at higher temperature and inhibitor concentration.

The adsorption of CBE and CBEK on metal surface obey Langmuir adsorption isotherm. The apparent activation energy (E_{a}) and heat of adsorption (Q_{ads}) are support the chemisorption process. While the free energy of adsorption (ΔG_{ads}), support both the physical adsorption and chemisorption are spontaneous exist, and chemisorption plays a key role at higher temperature.

CONFLICT OF INTEREST

The authors confirm that this article content has no conflict of interest.

ACKNOWLEDGEMENTS

The authors acknowledge the support of the National Natural Science Foundation of China (Grant No. 51101066) and the Analytical and Testing Center of the Huazhong University of Science and Technology.

REFERENCES

[1] Al-Otaibia MS, Al-Mayoufa AM, Khana M, *et al*. Corrosion inhibitory action of some plant extracts on the corrosion of mild steel in acidic media. Arab J Chem doi:10.1016/j.arabjc.2012.01.015.

[2] Abboud Y, Abourriche A, Ainane T, Hammouti, *et al*. Corrosion inhibition of carbon steel in acid media by bifurcaria bifurcata extract. Chem Eng Commun 2009; 196: 788-800.

[3] Orubite KO, Oforka NC. Inhibition of the corrosion of mild steel in hydrochloric acid solutions by the extracts of leaves of Nypa fruticans Wurmb. Mater Lett 2004; 58: 1768-72.

[4] Okafor PC, Liu CB, Zhu YJ, Zheng YG. Corrosion and corrosion inhibition behavior of N80 and P110 carbon steels in CO_2-saturated simulated formation water by rosin amide imidazoline. Ind Eng Chem Res 2011; 50: 7273-81.

[5] Satapathy AK, Gunasekaran G, Sahoo SC, Amit K, Rodrigues PV. Corrosion inhibition by Justicia gendarussa plant extract in hydrochloric acid solution. Corros Sci 2009; 51: 2848-56.

[6] Gece G. Drugs: A review of promising novel corrosion inhibitors. Corros Sci 2011; 53: 3873-98.

[7] Aramaki K, Hackerman N. Inhibition mechanism of medium-sized polymethyleneimine. J Electrochem Soc 1969; 116: 68-574.

[8] Ebenso EE. Synergistic effect of halide ions on the corrosion inhibition of aluminium in H_2SO_4 using 2-acetylphenothiazine. Mat Chem Phys 2003; 79: 58-70.

[9] Eduok UM, Umoren SA, Udoh AP. Synergistic inhibition effects between leaves and stem extracts of Sida acuta and iodide ion for mild steel corrosion in 1 M H_2SO_4 solutions. Arabi J Chem 2012; 5: 325-37.

[10] Tao P, Wang JB. Identification and characterization of transcripts differentially expressed during embryogenesis in *Capsella bursa-pastoris*. Biologia Plantarum 2012; 56: 415-21.

[11] Grosso C, Vinholes J, Silva LR, *et al.* Chemical composition and biological screening of *Capsella bursa-pastoris*. Rev Bras Farmacogn Braz J Pharmacogn 2011; 21: 635-44.

[12] Bekker A, Sorour K, Miller S. The use of cardioselective β-blockers in a patient with idiopathic hypertrophic subaortic stenosis and chronic obstructive pulmonary disease. J Clin Anes 2002; 14: 589-91.

[13] Ivanova D, Gerova D, Chervenkov T, Yankova T. Polyphenols and antioxidant capacity of Bulgarian medicinal plants. J Ethnopharm 2005; 96: 145-50.

[14] Szauer T, Brandt A. Adsorption of oleates of various amines on iron in acidic solution. Electrochimica Acta 1981; 26: 1253-6.

[15] Bastos AC, Ferreira MGS, Simões AMP. Effects of mechanical forming on the corrosion of electrogalvanised steel. Corros Sci 2013; 69: 87-96.

[16] Orazem ME, Tribollet B. Electrochemical Impedance Spectroscopy. New Jersey: John Wiley & Sons, Inc. 2008; pp. 236: the equation 13.9.

[17] Brug GJ, Van den Eeden ALG, Sluyters-Rehbach M, Sluyters JH. The analysis of electrode impedances complicated by the presence of a constant phase element. J Electroanal Chem 1984; 176: 275-95.

[18] Yan Y, Li W, Cai L, Hou B. Electrochemical and quantum chemical study of purines as corrosion inhibitors for mild steel in 1 M HCl solution. Electrochimica Acta 2008; 53: 5953-60.

[19] Mallaiya K, Subramaniam R, Srikandan SS, *et al.* Electrochemical characterization of the protective film formed by the unsymmetrical Schiff's base on the mild steel surface in acid media. Electrochimica Acta 2011; 56: 3857-63.

[20] Wang DH, Bu XZ, Gan FX, Zou JY, Yao LA. A differential polarization curve method and its application in anodic desorption

study of corrosion inhibitor. Corros Sci Protect Technol 1999; 01: 32-6.

[21] Drazic DM, Drazic VJ, Jevtic V. The slow adsorption of halide ions and some organics and their influence on corrosion rate determination from polarization data. Electrochimica Acta 1989; 34: 1251-7.

[22] Li XH, Deng SD. Inhibition effect of Dendrocalamus brandisii leaves extract on aluminum in HCl, H_3PO_4 solutions. Corros Sci 2012; 65: 299-308.

[23] Yurt A, Ulutas S, Dal H. Electrochemical and theoretical investigation on the corrosion of aluminium in acidic solution containing some Schiff bases. App Sur Sci 2006; 253: 919-25.

[24] Oguzie EE, Onuchukwu AI, Okafor PC, Ebenso EE. Corrosion inhibition and adsorption behaviour of Ocimum basilicum extract on aluminium. Pigm Resin Technol 2006; 35: 63-70.

[25] Bentiss F, Traisnel M, Gengembre L, Lagrenée M. A new triazole derivative as inhibitor of the acid corrosion of mild steel: electrochemical studies, weight loss determination, SEM and XPS. App Sur Sci 1999; 152: 237-49.

[26] Okafor PC, Liu CB, Zhu YJ, Zheng YG. Corrosion and corrosion inhibition behavior of N80 and P110 carbon steels in CO_2-saturated simulated formation water by rosin amide imidazoline. Ind Eng Chem Res 2011; 50: 7273-81.

[27] Lagrenee M, Mernari B, Bouanis M, Traisnel M, Bentiss F. Study of the mechanism and inhibiting efficiency of 3,5-bis(4-methylthiophenyl)-4H-1,2,4-triazole on mild steel corrosion in acidic media. Corros Sci 2002; 44: 573-88.

[28] Oguzie EE. Evaluation of the inhibitive effect of some plant extracts on the acid corrosion of mild steel. Corros Sci 2008; 50: 2993-8.

[29] Murakawa T, Nagaura S. Coverage of iron surface by organic compounds and anions in acid solutions. Corros Sci 1967; 7: 79-89.

[30] Grosso C, Vinholes J, Silva LR, *et al*. Chemical composition and biological screening of *Capsella bursa-pastoris*. Rev Bras Farmacogn Braz J Pharmacogn 2011; 21: 635-44.

[31] Wei X. Studies on the chemical constituents of domestic-made *Capsella bursa-pastoris* (L.); Master diss., Dept. of medic. Shenyang Pharmaceutical University 2007.

[32] Liu JP. The characteristics and high yield plant technology of *Capsella bursa-pastoris*. Mod Agr Sci Tech 2010; 10: 126.

[33] De Souza FS, Spinelli A. Caffeic acid as a green corrosion inhibitor for mild steel. Corros Sci 2009; 51: 642-9.

[34] Gunasekaran G, Chauhan LR. Eco friendly inhibitor for corrosion inhibition of mild steel in phosphoric acid medium. Electrochimica Acta 2004; 49: 4387-95.

[35] EL-Gaber AS, Fouda AS, EI Desoky AM. Synergistic inhibition of zinc corrosion by some anions in aqueous media. Ciência Tecnologia dos Materials 2008; 20: 71-7.

[36] Musa AY, Mohamad AB, Kadhum AAH, Takriff MS, Tien LT. Synergistic effect of potassium iodide with phthalazone on the corrosion inhibition of mild steel in 1.0 M HCl. Corros Sci 2011; 53: 3672-7.

[37] Bentiss F, Traisnel M, Lagrenee M. The substituted 1, 3, 4-oxadiazoles: a new class of corrosion inhibitors of mild steel in acidic media. Corros Sci 2000; 42: 127-46.

[38] Mayakrishnan G, Pitchai S, Raman K, Vincent AR, Nagarajan S. Inhibitive action of Clematis gouriana extract on the corrosion of mild steel in acidic medium. Ionics 2011; 17: 843-52.

Received: November 19, 2013 Revised: April 13, 2014 Accepted: May 5, 2014